Journal of Parasitology 2021 107(5) 731–738

Published 20 September 2021

DOI: 10.1645/21-2

Contents and archives available through www.bioone.org or www.jstor.org

Journal of Parasitology

journal homepage: www.journalofparasitology.org

QUANTIFYING BILATERAL INFECTION PATTERNS IN THE TREMATODE *ALLOGLOSSIDIUM RENALE*

Jenna M. Hulke[1], William H. Ellenburg[1], Derek A. Zelmer[2], and Charles D. Criscione[1]

[1] Department of Biology, Texas A&M University, 3258 TAMU, College Station, Texas 77840.
[2] Department of Biology and Geology, University of South Carolina Aiken, Aiken, South Carolina 29801.
Correspondence should be sent to Jenna M. Hulke at: *jhulke@bio.tamu.edu*

KEY WORDS

Bilateral asymmetry
Paired organs
Trematoda
Alloglossidium renale
Software
Monte Carlo simulation
Antennal gland
Decapoda
Palaemonetes kadiakensis

ABSTRACT

Within-host distributions of parasites can have relevance to parasite competition, parasite mating, transmission, and host health. We examined the within-host distribution of the adult trematode *Alloglossidium renale* infecting the paired antennal glands of grass shrimp. There are 4 possible parasite distributions for infections of paired organs: random, uniform, biased aggregation to 1 particular organ (e.g., left vs. right), or inconsistently biased (aggregated, but does not favor 1 side). Previous work has shown that morphological asymmetries in hosts can lead to biased infections of paired organs. Apparent symmetry between the antennal glands of grass shrimp leads to the prediction that there would be no bias for 1 particular organ. However, an alternative prediction stems from the fact that *A. renale* is hermaphroditic: aggregation between glands would increase outcrossing opportunities and thus, avoid inbreeding via self-mating. Existing methods to test for an overall pattern did not apply to the *A. renale* system because of low-intensity infections as well as many 0 values for abundance per unit of the antennal gland. Hence, we used Monte Carlo simulations to determine if the observed overall patterns differed from those expected by randomly allocating parasites into groups of 2. We found that in 3 of 4 data sets, *A. renale* infections did not deviate from random distributions. The fourth data set had a more uniform pattern than expected by chance. As there was no aggregation between glands and the proportion of worms in single gland infections did not differ from that expected by chance alone, we found no evidence of inbreeding avoidance as might be manifested via a within-host distribution. Given the large proportion of worms in single infections, we predict as a major evolutionary outcome that populations of *A. renale* will be largely inbred.

Distributions of parasites within individual hosts have been studied for their relevance to parasite intraspecific or interspecific competition (Holmes, 1973), niche restriction as a means to promote parasite mating (Rohde, 1979), impacts on host physiology or fitness (Karvonen and Seppala, 2008), and efficiency of parasite transmission (Pigeault et al., 2020). Within a host, parasites can be distributed continuously (e.g., encystment of larvae throughout the host body) or in discrete habitats (e.g., a specific organ). The latter is intriguing when the discrete habitat is a paired organ/structure (e.g., eyes, lungs, kidneys) of a bilateral host because of the potential further division of an infrapopulation (all the parasites of a given species within a host; Bush et al., 1997) into isolated habitat units. Isolation among parasites within hosts can influence the ecology or evolution of the host and/or parasite, creating a need to characterize within-host parasite distributions (Zelmer and Seed, 2004).

Infection patterns of paired organs among bilateral host organisms were recently reviewed by Johnson et al. (2014) wherein they highlighted possible causes and/or consequences for 4 possible distributional patterns: random, consistent bias, inconsistent bias, and uniform. A random pattern occurs when chance dictates infection of the paired organ and would result in the expectation of no difference in the mean abundance per unit of the paired organ (across samples of many pairs). Here, abundance is defined as the number of parasites in an organ unit of the pair (as opposed to a single host, sensu Bush et al., 1997) whether or not that organ unit is infected. A consistent bias is when 1 of the units of the pair has a higher mean abundance across all hosts. For example, echinostome metacercariae showed an infection bias with a higher mean abundance in the right versus left kidney of amphibians (Johnson et al., 2014). In this larval trematode–amphibian system, the bias was attributed to a host morphological asymmetry, where cercariae entering the cloaca first encountered the further descended right kidney (Johnson et al., 2014). Inconsistent bias indicates parasites are aggregated in 1 unit of a paired organ of a single host, but across hosts, there is no

association with a particular unit of the paired organ. Hence, the mean abundance per unit can be the same between the components of the paired organ. Whether consistently or inconsistently biased, aggregation of parasites into a unit of a paired organ has been hypothesized as a means to reduce the cost of infection as 1 component of the paired organ remains functional (Thiemann and Wassersug, 2000; Johnson et al., 2014). Lastly, a uniform distribution is when both organ units of the pair are simultaneously, evenly infected, resulting in no difference in the mean abundance per unit.

Among digenean trematodes, studies on infection distributions of paired organs have mostly focused on metacercarial stages: echinostomes in amphibian kidneys and diplostomids in the eyes of fish (reviewed in Johnson et al., 2014). These studies have largely centered on host-centric causes (e.g., asymmetric host morphology) and/or consequences (e.g., host health) of the distributional patterns. Little attention has been given to how adult trematodes are distributed in their paired habitats, even though many species of trematodes infect paired organs as adults (e.g., *Paragonimus* spp. [lungs of mammals], *Philophthalmus* spp. [eyes of birds], *Halipegus* spp. [Eustachian tubes of frogs], *Allocorrigia filiformis* [antennal glands of decapods], and *Troglotrema acutum* [nasal cavity of mustelids]). Indeed, in the review by Johnson et al. (2014), there is only a single study listed on adult trematodes; a descriptive survey on *Haematoloechus* spp. in the lungs of frogs (Whitehouse, 2002). Unfortunately, there are no more within-host, bilateral infection data for trematodes at the adult stage because more parasite-centric factors such as interference competition or mating systems may drive or be impacted by the infection distribution of adults between the units of a paired organ. For example, the selfing rates of tapeworms declined as infection intensity increased (Detwiler et al., 2017). Therefore, even though a host may have a high infection intensity, separation of adults between the components of a paired organ could act to increase selfing rates.

To contribute to the base knowledge on paired-organ infection dynamics at the adult stage in trematodes, we studied the within-host distribution of *Alloglossidium renale*, which as adults, infects the paired antennal glands of the Mississippi grass shrimp *Palaemonetes kadiakensis* (Font and Corkum, 1975). The parasite is hermaphroditic and, based on the presence of gravid adults in single infections (Suppl. Data, Fig. S1), we believe it is reasonable to assume it is self-compatible. Adults grow to a size of 2.8×1.1 mm and can fill the antennal gland (Fig. S1) to the point that little organ tissue remains (see figures in Landers and Jones, 2009). Despite the host tissue damage, grass shrimp can outlive the infection, as evidenced by decomposing worms or clusters of eggs found in antennal glands (Font and Corkum, 1976; Landers and Jones, 2009). The mollusc host of *A. renale* is not known, but field exposure experiments show that cercariae infect the shrimp and develop into adults in the antennal glands without the formation of a cyst (Font and Corkum, 1976). Published reports of *A. renale* include only locations in southern Louisiana (Font and Corkum, 1976, 1977) and southern Alabama (Landers and Jones, 2009). Our study includes new geographic locations in Mississippi and Texas (see Methods). Prevalence data from southern Louisiana indicate seasonal infections with peak prevalences of 60 to 70% from May through July with a sharp drop in August (Font and Corkum, 1977).

We had 2 a priori competing predictions for the distribution between the 2 antennal glands: random vs. aggregated. First, the antennal glands, like vertebrate kidneys (as in the echinostome–amphibian system discussed above), are part of the excretory system (De Gryse et al., 2020), but the nephritic system of decapods have 2 release openings (nephropores) at the base of the third body segment (Freire et al., 2008). It is not known if *A. renale* enters the nephropores, but a recent study found viral and bacterial pathogens can enter via these excretory pores (De Gryse et al., 2020). We are unaware of any reported morphological asymmetries in antennal glands, and with separate points of entry for each antennal gland (or multiple if cercariae can penetrate across the host's tegument), the prediction of a random infection pattern is reasonable. However, an alternative prediction of an aggregated pattern (biased or inconsistent) is still plausible if within-host aggregation still reduces host pathology by leaving 1 excretory gland operational. In addition, given that the adult stage infects the glands, the parasite's mating system could play a role in aggregating parasites (Rohde, 1979). As *A. renale* is hermaphroditic, individuals that end up as a single infection in 1 of the antennal glands would be forced to self-mate (i.e., they are subjected to extreme inbreeding). If there were negative fitness consequences from self-mating (i.e., inbreeding depression), then there could be selection on existing parasite traits (e.g., excretory–secretory chemical attractants; Fried, 1986) to facilitate aggregation into an antennal gland unit or at minimum avoid single infections to avoid inbreeding.

MATERIALS AND METHODS

Field sampling

Palaemonetes kadiakensis were collected from 3 locations: a pond in Gus Engeling Wildlife Management Area in Texas (31°55′44.94″N, 95°53′16.74″W) on 11 April 2015; a standing water body off of the Tallahatchie River in Money, Mississippi (33°37′51.46″N, 90°6′23.13″W) on 17 May 2014 and again on 24 May 2018; and a small lake, called Whisky Bay, within a swamp in Louisiana (30°23′28.74″N, 91°20′49.56″W) on 6 June 2019. We note for the Texas 2015 data set that some hosts were collected without recording the left/right data, which are needed to determine if mean abundance is different between the left and right units. The Texas 2015 data set can still be used to determine if there is a uniform, random, or aggregated pattern, but if there is aggregation, we cannot determine if there is a consistent or inconsistent bias. All data sets are available in Suppl. Data 1.

Specimens were collected by dip net and kept in aerated water until they were dissected. Host length (tip of the rostrum to the end of the tail), host sex, intensity (i.e., the sum of worms between the 2 gland units), and abundance per gland unit were recorded. Prevalence was not recorded in the Mississippi 2014 or Texas 2015 data sets, as only infected hosts were targeted for a different set of studies on *A. renale* (the translucence of the shrimp enables visual verification of infection; Fig. S1). Thus, for the Mississippi 2018 and Louisiana 2019 data sets, we could estimate the population mean abundance (total number of parasites divided by the number of all collected hosts; Bush et al., 1997) and variance in abundance. These estimates were used to parameterize the unconstrained Monte Carlo simulations described below. In all data sets, we estimated the population mean intensities as the

total number of parasites divided by the number of infected hosts (Bush et al., 1997).

Monte Carlo simulations

We implemented Monte Carlo simulations to test the within-host distributions for the following 2 reasons: First, although generalized linear models (GLM) have utility in testing for a consistent bias and variables associated with such a bias (e.g., Johnson et al., 2014), random, uniform, and inconsistent bias distributions can result in no difference in the mean abundance per unit of the paired organ. Thus, a lack of significance in a GLM is not conclusive in ruling out the null hypothesis of a random infection pattern. Second, although replicated goodness-of-fit tests (chi-square or G-test) provide a means to test within-host distributions (Wayland and Chubb, 2016), there is increased Type I error when a total count (i.e., infection intensity) is less than 10 (discussed in McDonald, 2014). The intensities in our data set are all below 10 (see Results). In addition, because of the log transformation, the G-test cannot be applied to a host with a count of zero in a unit of a paired organ. Hence, data are either thrown out (i.e., removal of hosts with low intensities) in the replicated analysis, or worse, an overall parasite distribution cannot be tested (i.e., a total G-test is not possible with any zero counts in a unit). The Monte Carlo simulations we implement allow us to test for a uniform, random, or aggregated pattern as well as incorporate all data including hosts that have a single gland abundance value of 0.

We evaluated the Type I and Type II error rates of 3 metrics of aggregation for use in the Monte Carlo simulations; mean difference in abundance (DA), mean index of dispersion (ID), and the mean exact probability (EP) for the binomial distribution with $p = q$. To test for consistent bias, we measured in each host the difference in abundance (DA) between left and right glands (left abundance minus right abundance). The DA is averaged across infected hosts to provide a mean DA with an expectation of 0 if there is no bias in the left vs. right gland. ID is the variance to mean ratio of the abundance per gland unit for each host. The mean ID is then calculated across infected hosts with an expectation of 1 for random, greater than 1 if aggregated, and less than 1 tending towards uniform. The EP takes on lower values for more aggregated patterns as compared to more uniform. For example, an aggregated pattern of 4 in the left gland and 0 in the right has a probability of 0.0625, whereas a uniform pattern of 2 and 2 has a probability of 0.375. The mean EP is calculated across infected hosts, but because the exact probabilities vary depending on the total intensity, the expectation changes with different among-host intensity distributions.

To examine the Type I error rate associated with the 3 metrics of aggregation, 50 draws, representing 50 hosts, were made from a negative binomial distribution for all combinations of a range of mean abundances (2, 3, and 4) and variance to mean ratios (1, 2, and 4). The resulting abundances were divided randomly into 2 groups (representing paired organs) within each host. The values of each metric were calculated and compared as 1-tailed comparisons to a null distribution of those values produced by repeating the randomization into 2 groups on the 50 abundances 10,000 times. We kept track of whether the initial values of the metrics exceeded (mean ID and mean DA) or were less than (mean EP) the 1-tailed 95% quantile for the appropriate null distribution. This procedure was replicated 10,000 times for each combination of mean abundance and variance to mean ratio.

The Type II error rate was evaluated with the same combinations of mean abundances and variance to mean ratios similarly by comparing a biased distribution to a null distribution (produced as described above). The bias was generated within the 50 hosts by making all paired combinations equiprobable when randomly allocated into 2 groups, which increases the frequency of aggregated patterns relative to that expected by chance. This procedure also was replicated 10,000 times. Note that in evaluating the Type I and II error rates for mean DA, the absolute value of DA was used from each host, as we were interested in whether this metric could detect bias in general rather than directionality per se.

We ran constrained and unconstrained Monte Carlo simulations to test the within-host distributions of the sample collections. Constrained simulations only consider the observed among-host intensity distribution, and thus could be run on all 4 data sets. We held constant the observed intensity distribution of the sample including intensity values of 1. We then randomly allocated parasites into the left and right glands creating 10,000 simulated data sets for the null distribution of each metric. We compared each observed metric to its respective null distribution.

Unconstrained simulations used the among-host abundance distribution and so explored a broader range of infection patterns. Unconstrained simulations were used on the Mississippi 2018 and Louisiana 2019 data sets. We simulated an abundance distribution by allocating parasites among hosts using a negative binomial parameterized with the observed number of hosts in the collections along with the observed mean abundance and variance in abundance. We ran this simulation 10,000 times and each time, parasites within hosts were randomly allocated between the antennal glands. Observed metrics were compared to the null distribution (see Suppl. Data, Fig. S2, for a flowchart of the procedure).

For all 3 metrics, we determined if the observed mean values from the sampled data sets fell outside the 95% confidence intervals (CI) of the simulated distribution of means (i.e., a 2-tailed $P \leq 0.05$). We used the approximately median-unbiased confidence interval estimation of Hyndman and Fan (1996), Definition 8 (implemented using Type 8 with the 'quantile' function in the R stats package; R Core Team, 2020). Figure 1 explains the criteria for inference with regards to the simulated distributions of the test statistics (i.e., determination of whether the sampled data sets show uniform, random, consistent bias, or inconsistent bias patterns).

In all Monte Carlo simulations, we also counted the number of hosts with single infections (HSI). Individuals in single infections are forced to self-mate, so the pattern of single infections may have important genetic consequences. The single infection count includes both hosts with a total intensity of 1 as well as hosts that have a gland with an intensity of 1 (e.g., 3 in the left and 1 in the right). Note, a host with 1 in the left gland and 1 in the right is counted only once in the HSI test statistic. The unconstrained and constrained Monte Carlo simulations using the above test statistics have been implemented in a user-friendly web application available at: https://jhulke.shinyapps.io/Distributional_patterns.

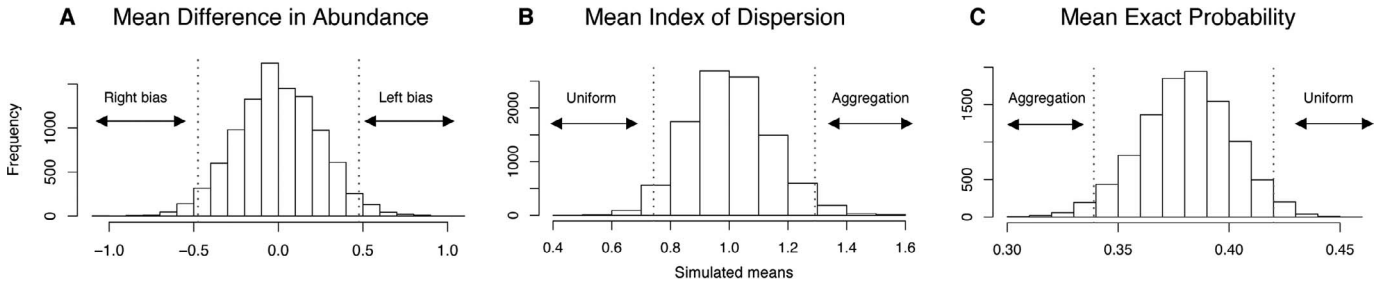

	Inferences			
Test statistics	Random	Uniform	Consistent bias	Inconsistent bias
Mean difference in abundance	Not significant	Not significant	Left or right bias	Not significant
Mean index of dispersion*	Not significant	Uniform	Aggregation	Aggregation

*Mean index of dispersion is testing the same patterns of aggregation and uniformity as the mean exact probability. Note that while both mean index of dispersion and the mean exact probability can detect both aggregation and uniformity, the zone of inference is reversed.

Figure 1. (**A**)–(**C**) Inference of bilateral infection patterns from the Monte Carlo simulations. The histograms provide example unconstrained null distributions of the 3 metrics where the dotted lines indicate the 95% confidence intervals. Observed metrics falling within these confidence intervals are not significant from that expected by random chance alone. The zones outside the confidence intervals indicate where observed metrics would be deemed significant. Indicated in these zones is the inference itself. The table indicates the dual criteria needed to determine if a bilateral infection is random, uniform, consistent bias, or inconsistent bias. See the main text for an explanation of the metrics themselves.

Test on abundance per gland unit

We performed a generalized linear mixed model (GLMM; family = Poisson) where the response variable was abundance per gland unit. The antennal gland unit (left vs. right) was the explanatory variable. We included 2 covariates, host length, and host sex, along with 2-way interactions between the explanatory variable gland unit and each of the covariates. The model also included the random effects of sample (i.e., the combined location and date data sets) and host individual nested within sample. The GLMM was performed in R (R Core Team, 2020) with the package *lme4* (Bates et al., 2015) used to fit restricted maximum-likelihood models. The 'Anova' function from the 'car package' (Fox and Weisberg, 2019) was used to test the significance of the fixed effects using the Type II Wald chi-square tests. The GLMM included all infected hosts from each sample except for the Texas 2015 data set, where we only used the subset of samples that had left/right information.

RESULTS

The Texas and Mississippi locations represent new geographic locations for *A. renale* and extend the known range west (about 430 km) and north (about 170 km), respectively, of previously published locations. Table I provides population-level summary data from the 4 locations. Prevalence (76 and 77%) and mean abundance (1.6 and 1.8) were similar between the Mississippi 2018 and Louisiana 2019 data sets, respectively. Mean intensities (1.85 to 2.58) were similar across all 4 locations. The prevalence data were comparable to that of Font and Corkum (1976), who reported between 60 and 70% prevalence from 2 locations in the peak months of May to July.

Evaluation of Monte Carlo test statistics

Over a range of parameter values similar to our observed data sets, the mean DA had a higher Type I error rate than mean ID or mean EP (Fig. 2A). The mean EP was overly conservative (higher Type II error) relative to mean DA and mean ID (Fig. 2B). Based on these results, we do not report further on the mean EP. The mean DA was retained to examine consistent bias.

Monte Carlo simulation results

In the constrained simulations, the Mississippi 2018 data set did not show significance for mean DA but did have a significantly lower mean ID (Table II). Hence, the inference was a uniform pattern. A random pattern was inferred for the remaining 3 data sets, as the mean DAs and mean IDs were not significant. The Texas 2015 data set tended to a uniform pattern with a mean ID less than 1 (0.843), but the 2-tailed *P*-value was 0.204 (calculated as 2 times the proportion of values $\leq$0.843). None of the data sets showed a deviation with regards to HSI (Table II).

In the unconstrained simulations, both the Louisiana 2019 and Mississippi 2018 data sets (Fig. 3) were robust with the results from the constrained models. The inference for Louisiana 2019 remained a random pattern and Mississippi 2018 remained a uniform pattern. There was no deficiency of single infections in either of these 2 data sets (HSI test statistic; Fig. 3).

Test on abundance per gland unit

In the GLMM, the random effects accounted for little to no variance. None of the 2-way interactions between gland unit and the covariates were significant. After removing the interaction terms, none of the variables, including gland unit, were significant (Table III). Hence, there was no evidence of a consistent gland unit bias or that host size and sex were associated with gland unit abundance. We repeated the analyses removing the random effects in a GLM and found the same results (data not shown).

DISCUSSION

Bilateral infection pattern

We had 2 a priori predictions for how *A. renale* might be distributed between the paired antennal glands. First, if the

Table I. Population-level summary data of hosts and parasites collected from the 4 sampling locations.

Location (n*)	Prevalence	Mean abundance (variance)	Mean intensity (range)	Sum of parasites in left gland	Sum of parasites in right gland
Louisiana 2019 (58)	0.776	1.84 (2.73)	2.38 (1–6)	52	55
Mississippi 2018 (126)	0.762	1.63 (2.03)	2.14 (1–7)	101	104
Mississippi 2014 (31)	NA†	NA	2.58 (1–9)	37	43
Texas 2015 (39)	NA	NA	1.85 (1–5)	NA	NA

* n is the number of hosts sampled. In the Louisiana 2019 and Mississippi 2018 data sets, n includes noninfected hosts, whereas in the other 2 data sets, n is only infected hosts.

† Prevalence was not ascertained from Mississippi 2014 or Texas 2015, as hosts were selected for visible signs of infection. Also, left–right information was not recorded from all hosts collected from Texas 2015.

mating system was driving the distributional patterns, we expected to find aggregation. We found no evidence of a consistent bias in the GLMM or the Monte Carlo analyses. More broadly, the Monte Carlo tests showed no evidence of aggregation. Thus, even though *A. renale* is hermaphroditic, no aggregation could serve to facilitate outcrossing opportunities. In addition, with HSI used as a test statistic in the Monte Carlo simulations, we did not detect a deficiency of hosts with single infections. Hence, there was no within-host pattern that might suggest parasites were avoiding inbreeding.

Our alternate prediction was that *A. renale* would be randomly distributed, as there is no known host asymmetry between the left and right antennal glands (each with a possible point of entry). Three of 4 data sets did not have a mean ID deviating from random. However, Mississippi 2018, the data set with the largest sample size (Table I), showed a significant tendency towards a uniform distribution. This result was robust with regard to using an unconstrained or constrained Monte Carlo simulation. Furthermore, the Texas 2015 data set, although not significantly departing from random, had an observed mean ID (0.843; Table II) trending towards a uniform distribution (only 10.2% of simulated values were less than or equal to the observed). Overall, we conclude that *A. renale* displays a random infection pattern. Additional samples are needed to determine the robustness of the possible tendencies to a uniform pattern that we observed in our samples.

The only parasite systems reported by Johnson et al. (2014) to have uniform distributions are mites on the body surface of insects (Cooper, 1954; McLachlan et al., 2008). These studies discussed how aggregated distributions might hinder the flight ability of the insect host and therefore, how "symmetrical" infections might least impair host flight. However, Cooper (1954) only provides descriptive arguments but provides no formal analysis. McLachlan et al. (2008) found a bimodal distribution where there was an excess of hosts with a uniform pattern of infection and excess with aggregation. Hence, the classification of this system as uniform may be an oversimplification.

In another mite study, Cross and Bohart (1969) reported 1 significant asymmetrical and 4 nonsignificant replicated chi-square tests from 5 subsets of data sets (see their table 1). They concluded an overall symmetrical distribution. Herein, we note a semantic problem with the term "symmetry" as both a uniform

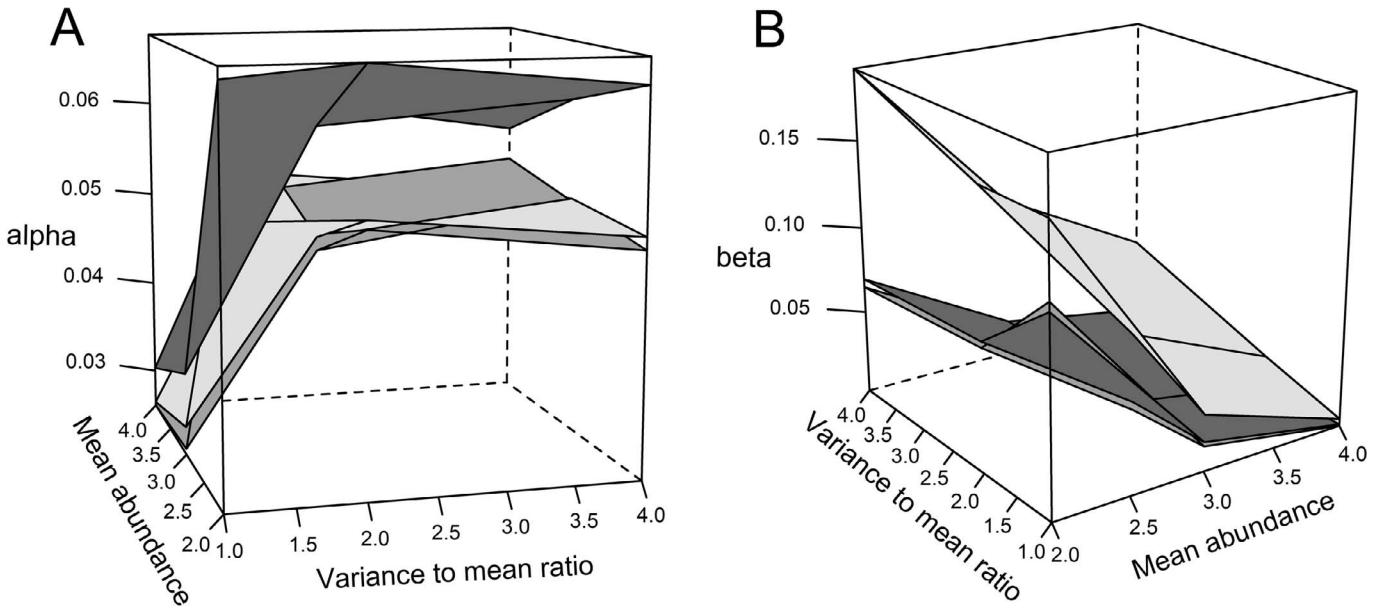

Figure 2. Error rates for mean difference in abundance (DA; dark gray), mean index of dispersion (ID; medium gray), and mean exact probability (EP; light gray) based upon 10,000 random and biased pairwise distributions for 50-host samples drawn from negative binomial distributions with a range of mean abundances (2, 3, and 4) and variance to mean ratios (1, 2, and 4). (**A**) Type I error rate (alpha). (**B**) Type II error rate (beta).

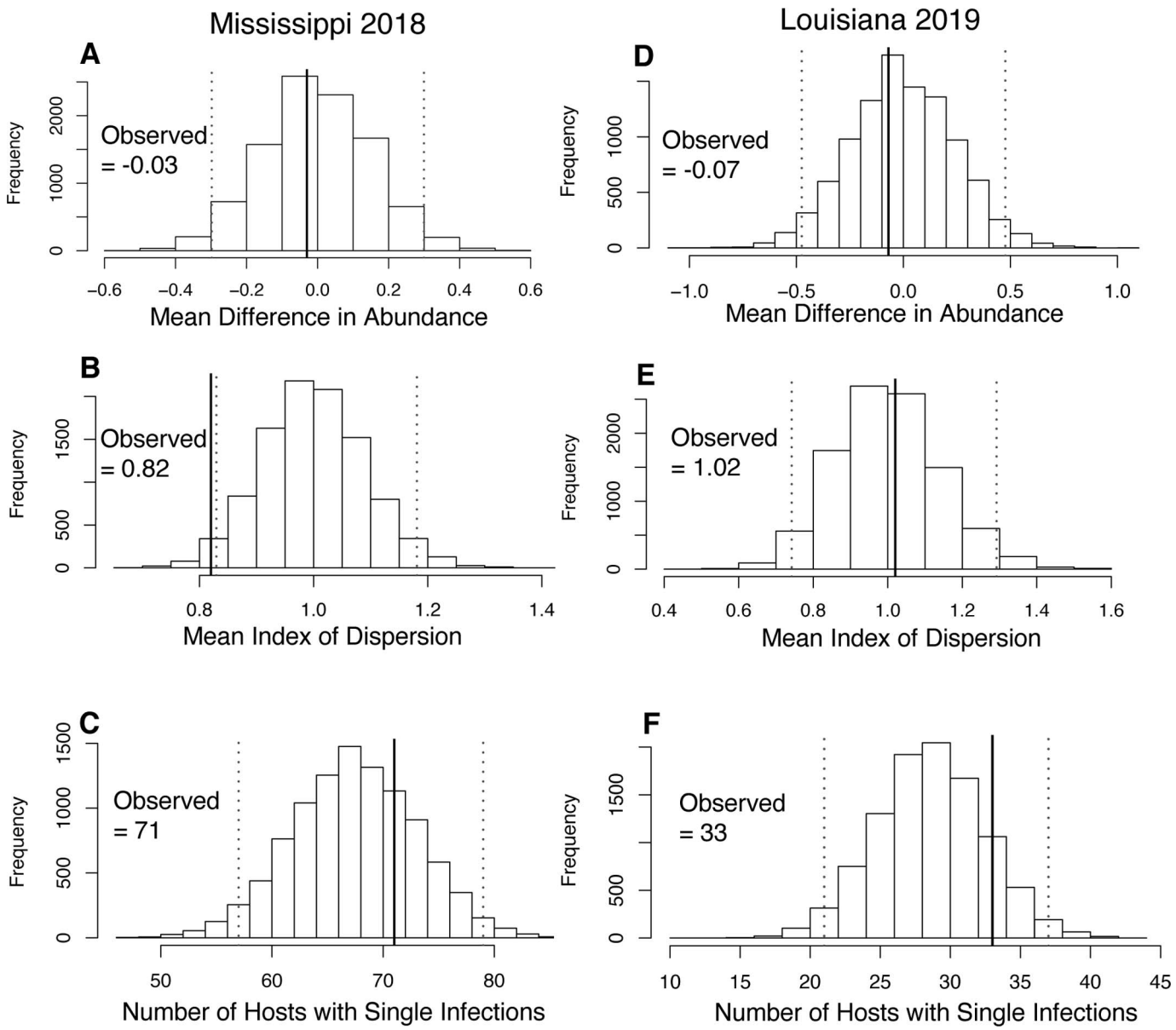

Figure 3. Results from unconstrained Monte Carlo simulations. Dotted lines indicate 95% confidence intervals and the solid lines indicate observed values of the test statistics. (**A**)–(**C**) Results for Mississippi 2018 data set. (**D**)–(**F**) Results from Louisiana 2019 data set. The Mississippi 2018 data set shows a more uniform pattern than expected by chance.

Table II. Results from the constrained Monte Carlo simulations.

Population	Observed no. of single infections*	Observed mean difference in abundance	Observed mean index of dispersion	Inferred distribution
Louisiana 2019	33 (31.6)	−0.066	1.02	Random
Mississippi 2018	71 (70.4)	−0.031	0.815‡	Uniform
Mississippi 2014	21 (19.7)	−0.194	1.012	Random
Texas 2015	31 (28.8)	NA†	0.843	Random

* In parentheses is the mean number of hosts with single infections across the simulations.
† The difference in abundance could not be ascertained in the Texas 2015 data set (see Materials and Methods).
‡ Significant at $P \leq 0.05$ based on a 2-tailed analysis (i.e., the observed value fell outside the 95% confidence interval of the simulation).

Table III. Generalized linear mixed model results testing for an association with the response variable, abundance per gland unit. Two-way interactions with gland unit and the covariates were not significant, and thus were removed from the model.

Fixed effect	Estimate	Chi-square value	df	*P* value
Gland unit	0.063	0.409	1	0.52
Host length	−0.006	0.185	1	0.67
Host sex	0.155	1.728	1	0.19
Random effects			Variance	
location–date:host.id			0	
location–date			7.56e-4	

and random distribution between units of a paired structure are deemed "symmetrical" for failing to reject the 1:1 ratio of the total test in a replicated goodness-of-fit test. Upon reexamination of the results in Cross and Bohart (1969), 1 test showed aggregation, 3 were random, and 1 had a significant uniform pattern (df =15 and total chi-square = 6.22 yields $P = 0.975$, which is significantly more uniform than expected given the *P*-value is extreme in the other direction). Overall, we did not find quantitative support for uniform patterns within the existing studies on mites. Although it is clear from experimental work that unequal bilateral mite loads can impair host flight performance (McLachlan et al., 2008), it remains to be determined if such a pressure induces uniform over random distributional patterns in nature.

If uniform patterns are found in future studies of *A. renale*, there would be some interesting hypotheses to test. For example, 1 hypothesis is analogous to the mite–insect systems, where the swimming performance of the grass shrimp could be negatively impacted by the aggregation of *A. renale* in the antennal glands if an uneven load between the glands impacted grass shrimp balance. However, more research is needed to understand the effect *A. renale* has on both the swimming ability and the pathology of the host. Taken from the parasite's point of view, another hypothesis is that intraspecific competition may be driving a uniform distribution especially given that an adult *A. renale* is about the size of an antennal gland itself (Fig. S1).

Across all data sets and examining intensities ≥ 2, there were 110 worms out of the total 381 that occurred in a unit of an antennal gland by themselves. This result underscores how infections of paired organs can impact parasite evolutionary dynamics by precluding outcrossing opportunities between parasites even though they infect the same host. In the case of *A. renale*, such a high proportion of worms in single infections could lead to high selfing rates. Hence, from an evolutionary perspective, a predictive consequence is that *A. renale* exists in highly inbred populations.

The only other system in which the paired organ distribution pattern of adult trematodes has been examined was with *Haematoloechus* spp. from the lungs of frogs (Whitehouse, 2002). Johnson et al. (2014) listed this pattern as random. Although this categorization agrees with a statement in the abstract, "There was no significant difference in prevalence or intensity of lung flukes with regard to right or left lung," the results presented separately for 2 fluke species indicate potential biases. In particular, Whitehouse (2002) states that there was a higher proportion of infections in the right lung for *H. longiplexus*, whereas *H. breviplexus* had a higher proportion in the left lung of the same host species. Unfortunately, data are not presented on a per-parasite-species basis, so the overall distributional patterns for each species of *Haematoloechus* are unclear.

Brief comments on the Monte Carlo analysis

Given that existing methods to analyze bilateral infection patterns are limited to testing for a consistent bias (e.g., GLMs), or are limited to higher intensities and no 0 abundance per unit values (e.g., goodness-of-fit tests), the Monte Carlo simulations we presented should be a useful tool in facilitating future studies on bilateral infections. Over a range of parameters similar to the mean abundances and variances observed in our data, the mean ID performed well for both Type I and II errors. The mean ID, therefore, can be used to evaluate if an overall bilateral infection pattern is uniform, random, or aggregated in similar low-intensity data sets as that of *A. renale* without having to discard data (as compared to the G-test; Wayland and Chubb, 2016). The mean DA, however, had a slightly elevated Type I error (alpha = 0.06–0.07; Fig. 2A). In relation to our data sets, mean DA was not significant so the lack of directionality (i.e., no bias to 1 gland over the other) is a robust conclusion for *A. renale*. Nevertheless, it is worth exploring other test statistics that can inform about consistent bias to avoid Type I error. Additional evaluation at higher intensities would also be a useful endeavor to compare how the Monte Carlo simulations presented herein perform against the G-test in evaluating bilateral infection patterns.

ACKNOWLEDGMENTS

We thank E. Kasl, B. Trejo, and A. Sakla for assisting in field collections. We are grateful to H. Watts for help with transportation and use of land in Louisiana. This work was supported by the National Science Foundation, DEB 1655147 (CDC).

LITERATURE CITED

Bates, D., M. Mächler, B. Bolker, and S. Walker. 2015. Fitting linear mixed-effects models using lme4. Journal of Statistical Software 67: 1–48. doi:10.18637/jss.v067.i01.

Bush, A. O., K. D. Lafferty, J. M. Lotz, and A. W. Shostak. 1997. Parasitology meets ecology on its own terms: Margolis et al. revisited. Journal of Parasitology 84: 575–583.

Cooper, K. W. 1954. Venereal transmission of mites by wasps, and some evolutionary problems arising from the remarkable association of *Ensliniella trisetosa* with the wasp *Ancistrocerus antilope*. Biology of eumenine wasps II. Transactions of the American Entomological Society 80: 119–174.

Cross, E. A., and G. E. Bohart. 1969. Phoretic behavior of four species of alkali bee mites as influenced by season and host sex. Journal of the Kansas Entomological Society 42: 195–219.

De Gryse, G. M., T. Van Khuong, B. Descamps, W. Van Den Broeck, C. Vanhove, P. Cornillie, P. Sorgeloos, P. Bossier, and H. J. Nauwynck. 2020. The shrimp nephrocomplex serves as a major portal of pathogen entry and is involved in the molting process. Proceedings of the National Academy of Sciences of the United States of America 117: 28374–28383.

Detwiler, J. T., I. C. Caballero, and C. D. Criscione. 2017. Role of parasite transmission in promoting inbreeding: I. Infection intensities drive individual parasite selfing rates. Molecular Ecology 26: 4391–4404.

Font, W. F., and K. C. Corkum. 1975. *Alloglossidium renale* n. sp. (Digenea: Macroderoididae) from a fresh-water shrimp and *A. progeneticum* n. comb. Transactions of the American Microscopical Society 94: 421–424.

Font, W. F., and K. C. Corkum. 1976. Ecological relationship of *Alloglossidium renale* (Trematoda: Macroderoididae) and its definitive host, the freshwater shrimp, *Palaemonetes kadiakensis*, in Louisiana. American Midland Naturalist 96: 473–478.

Font, W. F., and K. C. Corkum. 1977. Distribution and host specificity of *Alloglossidium* in Louisiana. Journal of Parasitology 63: 937–938.

Fox, J., and S. Weisberg. 2019. An R Companion to Applied Regression, 3rd ed. Sage, Thousand Oaks, California, 608 p.

Freire, C. A., H. Onken, and J. C. McNamara. 2008. A structure–function analysis of ion transport in crustacean gills and excretory organs. Comparative Biochemistry and Physiology Part A: Molecular & Integrative Physiology 151: 272–304.

Fried, B. 1986. Chemical communication in hermaphroditic digenetic trematodes. Journal of Chemical Ecology 12: 1659–1677.

Holmes, J. C. 1973. Site selection by parasitic helminths: interspecific interactions, site segregation, and their importance to the development of helminth communities. Canadian Journal of Zoology 51: 333–347.

Hyndman, R. J., and Y. Fan. 1996. Sample quantiles in statistical packages. American Statistician 50: 361–365.

Johnson, P. T. J., J. Koprivnikar, S. A. Orlofske, B. A. Melbourne, and B. E. LaFonte. 2014. Making the right choice: Testing the drivers of asymmetric infections within hosts and their consequences for pathology. Oikos 123: 875–885.

Karvonen, A. and O. Seppala. 2008. Eye fluke infection and lens size reduction in fish: A quantitative analysis. Diseases of Aquatic Organisms 80: 21–26.

Landers, S. C., and R. D. Jones. 2009. Pathology of the trematode *Alloglossidium renale* in the freshwater grass shrimp *Palaemonetes kadiakensis*. Southeastern Naturalist 8: 599–608.

McDonald, J. H. 2014. Handbook of Biological Statistics, 3rd ed. Sparky House Publishing, Baltimore, Maryland, 299 p.

McLachlan, A. J., T. W. Pike, and J. C. Thomason. 2008. Another kind of symmetry: Are there adaptive benefits to the arrangement of mites on an insect host? Ethology Ecology & Evolution 20: 257–270.

Pigeault, R., J. Isaïa, R. S. Yerbanga, K. R. Dabiré, J. B. Ouédraogo, A. Cohuet, T. Lefèvre, and P. Christe. 2020. Different distribution of malaria parasite in left and right extremities of vertebrate hosts translates into differences in parasite transmission. Scientific Reports 10: 1–9.

R Core Team. 2020. R: A Language and Environment for Statistical Computing. R Foundation for Statistical Computing, Vienna, Austria.

Rohde, K. 1979. A critical evaluation of intrinsic and extrinsic factors responsible for niche restriction in parasites. American Naturalist 114: 648–671.

Thiemann, G. W., and R. J. Wassersug. 2000. Biased distribution of trematode metacercariae in the nephric system of Rana tadpoles. Journal of Zoology 252: 531–547.

Wayland, M., and J. C. Chubb. 2016. A new R package and web application for detecting bilateral asymmetry in parasitic infections. Folia Parasitologica 63: 039.

Whitehouse, C. A. 2002. A study of the frog lung fluke *Haematoloechus* (Trematoda: Haematoloechidae) collected from areas of Kentucky and Indiana. Proceedings of the Indiana Academy of Science 111: 67–76.

Zelmer, D. A., and J. R. Seed. 2004. A patch hath smaller patches: Delineating ecological neighborhoods for parasites. Comparative Parasitology 72: 93–103.